

# Reynolds number calculation and applications for curved wall jets

Valeriu DRAGAN\*

\*Corresponding author

COMOTI – Romanian Gas Turbine Research and Development Institute  
220 D Iuliu Maniu Avenue, 061126 Bucharest 6, Romania, P.O. 76, P.O.B. 174  
drvaleriu@gmail.com

DOI: 10.13111/2066-8201.2014.6.3.4

**Abstract:** *The current paper refers to the preliminary estimation of the Reynolds number for curved wall jets. This, in turn, can be a useful tool for controlling the boundary layer mesh size near a generic curved wall which is wetted by a thin, attached jet. The method relies on analytical calculations that link the local curvature of the wall with the pressure gradient and further, the local Reynolds number. Knowing the local Reynolds number distribution, a CFD user can tailor their mesh size to more exact specifications (e.g.  $y^+=1$  for  $k$ - $\omega$  RANS models) and lower the risk that the mesh is too coarse or finer than necessary.*

**Key Words:** *Coanda effect, supercirculation,  $y^+$ , meshing, circulation control*

## NOMENCLATURE

$C$  = length of a curvilinear path  
 $C_p$  = pressure coefficient  
 $h$  = blowing wall jet slot height  
 $R$  = radius of curvature  
 $Re$  = Reynolds number  
 $Re_x$  = local Reynolds number  
 $Re_r$  = reduced Reynolds number  
 $u_j$  = jet initial velocity magnitude  
 $u_m$  = jet local magnitude  
 $y^+$  = non-dimensional wall distance  
 $\rho$  = fluid density  
 $\mu$  = fluid dynamic viscosity  
 $\theta$  = angular position [degrees]

## 1. INTRODUCTION

Current fluid dynamics practices include the extensive use of CFD calculations using RANS turbulence models. One of the (re)emerging technologies in the aerospace industry is the use of curved wall jets that entrain the free stream increasing the efficiency of bladed machinery Refs[1-3] or improving lift and drag of aircraft wings Refs [4-6] or other industrial applications [7-9].

Computational Fluid Dynamics of devices which use wall jets raises the problem of correctly estimating the cell size near the walls subject to the wall jet so that the turbulence model can perform optimally.

However, underestimating the first cell size can lead to prohibitive cell counts. A mesh that has a first cell too thin, will lead to more cells thus increasing the computational time and/or computational resources.

This is particularly problematic in cases such as supercirculation or entrainment airfoils which combine the free stream with a typically thin blowing wall jet region which has a high velocity jet.

This raises the problem of how to blend the two regions together while maintaining the same  $y^+$  requirements of the turbulence model.

For unstructured meshes this problem is overcome by interfacing the two regions into two separate domains, each having its own mesh.

The problem created by this approach is that an unstructured mesh tends to have more cells than a structured one and, hence, requires more CPU/hours.

Another problem, which theoretically can be eliminated through the use of improved mathematical models, is the information exchange between the two domains through the interface(s).

Practice has shown that the interface, in some cases (i.e. high Mach numbers near the interface), may lead to undesired - and often hard to spot - calculation errors.

On the other hand, a structured grid should have a sufficiently long blending zone between the higher cell size on the area which is not wetted by the wall jet and the wall jet region itself.

The transition between the two regions should have a cell size ratio low enough ( $\sim 1.2:1$ ) so that the numerical scheme would not become unstable.

Therefore, estimating the exact cell size in the high velocity, wall jet region would help minimize the overall mesh size and would also help with its smoothness.

## 2. THE LOCAL REYNOLDS NUMBER ESTIMATION

One of the first definitions for the Reynolds number in the case of a wall jet is given by T. Vit [10].

$$Re = \frac{u_j \sqrt{Rh} \rho}{\mu}, \quad (1)$$

Although more recent articles [11] provide an even simpler (and much more conservative) definition for the Reynolds number,

$$Re = \frac{u_j h \rho}{\mu}. \quad (2)$$

These definitions, although useful by factoring in the radius of curvature  $R$  and the initial thickness of the wall jet  $h$ , have the inconvenience that they do not account for the velocity variation across the ramp - which can be substantial.

Therefore, a more accurate definition, that correlates all the major factors influencing the jet wall flow, can prove useful in estimating the Reynolds number distribution across the curved wall.

### 2.1. The characteristic length and characteristic velocity estimations

In the case of a circular arc - which is the case of most entrainment airfoil applications - the simple geometric relation applies, where  $\theta$  is the angular span washed by the jet across the wall.

$$C = \pi R \frac{\theta}{180} \quad (3)$$

From the inviscid flow theory, the relation between the pressure gradient and the local curvature ratio can easily be estimated.

It must be said that this is merely an approximation since the applications for this calculation are related to turbulent flows, having a complexity that goes beyond the inviscid flow calculations. Considering the notations in Fig.1, the pressure gradient as a function of streamline curvature can be deduced.

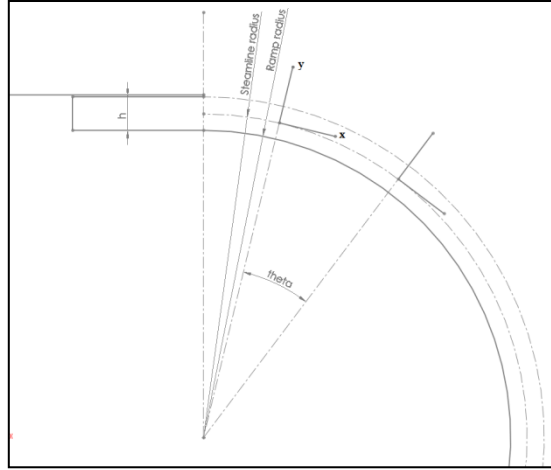


Fig.1 - The forces acting on a fluid subjected to a curved pathway

From the Oy momentum equation,

$$\frac{\partial P}{\partial y} = -\rho u \frac{\partial v}{\partial x} - \rho v \frac{\partial v}{\partial y} \quad (4)$$

where, considering the notations already made,

$$u = u_j \cos \theta \quad \text{and} \quad v = u_j \sin \theta$$

we can deduce that in the origin of the coordinate system ( $\theta=0$ ) the velocity components become  $v=0$  and  $u=u_j$ .

Since we know the mathematical relations,

$$\frac{\partial v}{\partial x} = \frac{\partial u_j}{\partial x} \sin \theta + u_j \frac{\partial \theta}{\partial x} \cos \theta = \frac{u_j}{R_c}, \quad (5)$$

we determine the pressure gradient as a function of the local curvature radius to be:

$$\frac{\partial P}{\partial y} = -\rho \frac{u_j}{R_c}. \quad (6)$$

where  $y$  is the local normal direction to the streamline.

It can be seen that for positive (convex) radii, the pressure gradient is adverse, whereas for the negative curvatures (concave) the pressure gradient is positive.

Knowing the pressure gradient, the local velocity can be calculated

$$u_m = u_j \sqrt{1 - C_p} \quad (7)$$

In the case of thin jet walls, Benner [12] gives the pressure coefficient estimate

$$C_p = -\frac{2h}{R} \tag{8}$$

Reference [13] presents two additional blending coefficients for the portion near the jet slot and, near the flow separation region, respectively.

$$F_1 = 0,6014 + 0,4056 \left\{ 1 - \exp \left[ -3,198 \left( \frac{\theta}{\frac{h}{R} \frac{180}{\pi}} \right) \right] \right\} \tag{9}$$

$$F_2 = 1,02915 - 0,02915 \cdot \exp \left( \frac{\theta - (\theta_{sep} - 0,143 \cdot \theta_{sep})}{(\theta_{sep} + 0,143 \cdot \theta_{sep}) - (\theta_{sep} - 0,143 \cdot \theta_{sep})} \right) \tag{10}$$

For a circular ramp, the local Reynolds number can be estimated at

$$Re_x = \frac{u_j \sqrt{1 + \frac{2h}{R}} \cdot \pi R \cdot \frac{\theta}{180} \rho}{\mu} \tag{11}$$

Figure 2 presents a comparison between the reduced Reynolds number ( $Re^*[\mu/u_j \cdot \rho]$ ) using the equations in Refs[10, 11] and Eq.(11).

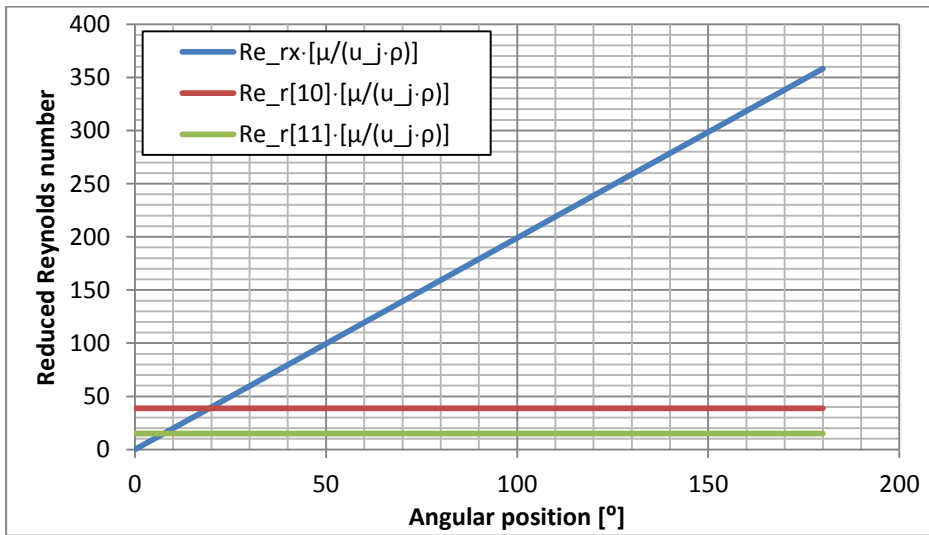


Fig. 2 - Local reduced Reynolds number estimate for a circular ramp R=100 and h=15

It should be noted that, for the lower angular positions, the reduced Reynolds number ( $Re^*[\mu/u_j \cdot \rho]$ ) proposed in this paper is actually lower than the ones proposed in papers [10] and [11].

This is not a natural behavior since the Reynolds number cannot be equal to zero. Hence a corrected version for Eq.11 is required:

$$Re_x = \frac{u_j \sqrt{1 + \frac{2h}{R}} \cdot \left( h + \pi R \cdot \frac{\theta}{180} \right) \rho}{\mu} \tag{12}$$

This adds the height of the slot to the specific length, shifting the graph of Eq.11 up with a factor of  $h$ .

## 2.2. Generalization

For a ramp defined by an arbitrary equation  $f(x)$  (which must be twice differentiable), one can determine the local pressure coefficient using the curvature radius analytical calculation. Also, one can analytically determine the length of the ramp which is “washed” by the jet. These two factors are described by Eqs.13-14.

$$R_{local} = \frac{\{1 + [f'(x)]^2\}^{3/2}}{f''(x)} \quad (13)$$

$$C = \int_0^x \sqrt{1 + [f'(x)]^2} dx \quad (14)$$

$$Re_x = \frac{u_j \sqrt{1 + \frac{2hf''(x)}{\{1+[f'(x)]^2\}^{3/2}} \cdot \left( h + \pi \int_0^x \sqrt{1 + [f'(x)]^2} dx \right) \rho}{\mu} \quad (15)$$

Note that, for the purposes of this paper, the effects of compressibility - hence the variation in density - will be neglected although, some applications use blowing flaps for supersonic flight control [14] or thrust vectoring [15].

## 3. POTENTIAL APPLICATIONS - CALCULATING THE FIRST CELL THICKNESS FOR CFD APPLICATIONS

Caution must be exercised when using the above calculation to estimate the first cell height near the wall. This is because, although the pressure gradient is typically well estimated, the calculation is still inviscid not turbulent.

A possible application of the above Reynolds number estimation is the calculation of the first cell size for a given  $y^+$  mesh near a wall. Reference[16] gives the following relations:

$$y_x = \frac{y^+ \cdot \mu}{\rho \cdot u_{*x}} \quad (16)$$

$$u_{*x} = \sqrt{\frac{\tau_{wx}}{\rho}} \quad (17)$$

$$\tau_w = C_{fx} \cdot \rho \cdot \frac{u_{mx}^2}{2} \quad (18)$$

$$C_{fx} = \frac{0.455}{(\log_{10} Re_x)^{2.58}} \quad (19)$$

An alternative calculation method is given by Ref [17]

$$y_x = 6 \left( \frac{u_{mx} \cdot \rho}{\mu} \right)^{-\frac{7}{8}} \left( \frac{x}{2} \right)^{\frac{1}{8}} y^+ \quad (20)$$

As a good practice, the recommendation of CFD experts (Ref [18] NASA) is to continue meshing the viscous sub-layer with constant cells and above it to have an expansion ratio as close to one unit as possible so that the numerical scheme and the CFD solution is not adversely influenced.

In order to meet these requirements it is useful to know the local thickness of the boundary layer. This, in turn requires for the user to know the velocity profile for each individual location. A good approximation can be calculated using the CEPA model Ref [13] which gives estimates to both the local maximal velocity  $u_m$  and the wall distance where it can be found  $y_m$ . Although technically the boundary layer thickness is considered to be the wall distance at which 99% of the free stream velocity is located, since this application refers to thin wall jets - which have an important variation between the initial,  $u_j$ , and the local maximal,  $u_m$ , velocities - a compromise can be made that the thickness of the boundary layer to be approximately equal to  $y_m$ . For general use however a good approximation for the turbulent boundary layer thickness can be made using the classical

$$\delta_x = \frac{0.382}{Re_x^{1/5}} \quad (21)$$

#### 4. CONCLUSIONS AND FURTHER WORK

Thus far the above calculations have been only theoretical in nature. Further work must validate the theoretical statements made herein through proper numerical CFD simulations.

Typically, flows subject to the Coanda effect are difficult to simulate with RANS turbulence models due to the curvature effects which may lead to exaggerated turbulence generation, see Ref [19] Newer models, however, incorporate curvature corrections and have test been-proven, see Ref [11].The continued research must present a comparative study performed with the Menter SST - RC Ref [20, 21 ] and the Spalart Allmaras RC Ref [22] models. Furthermore, it is important to correlate the computational simulations with the experimental research from the literature, see Refs [23-25].

#### REFERENCES

- [1] J. Yen, N. A. Ahmed, Enhancing vertical axis wind turbine by dynamic stall control using synthetic jets, *Journal of Wind Engineering and Industrial Aerodynamics*, Volume **114**, ISSN: 0167-6105, Pages 12–17, DOI: 10.1016/j.jweia.2012.12.015, March 2013.
- [2] K. Taylor, C. Leong, M. Amitay, *Dynamic Load Control on a Finite Span Wind Turbine Blade Using Synthetic Jets*, 50<sup>TH</sup> AIAA AEROSPACE SCIENCES MEETING INCLUDING THE NEW HORIZONS FORUM AND AEROSPACE EXPOSITION, 2012, doi/abs/10.2514/6.2012-894.
- [3] S. Wang, L. Cai, X. Zhou, S. Lu, Numerical investigation on effectiveness of flow separation control in two-dimensional high-load compressor cascade by synthetic jet, *Journal of Thermal Science*, ISSN: 1003-2169 (print version), ISSN: 1993-033X (electronic version), Volume **21**, Issue 5, pp 441-446, DOI: 0.1007/s11630-012-0566-x, October 2012.
- [4] K. Sommerwerk, M. C. Haupt, Design analysis and sizing of a circulation controlled CFRP wing with Coandă flaps via CFD–CSM coupling, *CEAS Aeronautical Journal*, ISSN: 1869-5582 (Print), ISSN: 1869-5590 (Online) Volume **5**, Issue 1, pp 95-108, DOI: 10.1007/s13272-013-0093-9, March 2014.
- [5] D. Keller, Numerical Approach Aspects for the Investigation of the Longitudinal Static Stability of a Transport Aircraft with Circulation Control, A. Dillmann et al. (eds.), *New Results in Numerical and Experimental Fluid Mechanics IX*, Notes on Numerical Fluid Mechanics and Multidisciplinary Design 124, DOI: 10.1007/978-3-319-03158-3\_2, © Springer International Publishing Switzerland 2014.
- [6] K. Sommerwerk, M. Haupt, P. Horst, Aeroelastic Performance Assessment of a Wing with Coanda Effect Circulation Control via Fluid-Structure Interaction, 31<sup>ST</sup> AIAA APPLIED AERODYNAMICS CONFERENCE, 2012, doi/abs/10.2514/6.2013-2791.

- [7] M. Trancossi and A. Dumas, *Coanda Synthetic Jet Deflection Apparatus and Control*, SAE Technical Paper 2011-01-2590, 2011, doi:10.4271/2011-01-2590.
- [8] A. Kourta, C. Leclerc, Characterization of synthetic jet actuation with application to Ahmed body wake, *Sensors and Actuators A: Physical*, Volume **192**, ISSN: 0924-4247, 1 April 2013, Pages 13–26, DOI: 10.1016/j.sna.2012.12.008.
- [9] D. A. Axinte, B. Karpuschewski, M.C. Kong, A. T. Beaucamp, S. Anwar, D. Miller, M. Petzel, High Energy Fluid Jet Machining (HEFJet-Mach): From scientific and technological advances to niche industrial applications, *CIRP Annals - Manufacturing Technology*, Available online, 19 June 2014, DOI: 10.1016/j.cirp.2014.05.001
- [10] T. Vit, *Experimental and Theoretical Study of Heated Coanda jet*, PhD thesis, 2004.
- [11] T. Nishino, S. Hahn, K. Shariff, *LES of high-Reynolds-number Coanda flow separating from a rounded trailing edge of a circulation control airfoil*, 8<sup>th</sup> International ERCOFTAC Symposium on Engineering Turbulence Modelling and Measurements (ETMM8), Marseille, France, 9-11 June, 2010.
- [12] S.I. Benner, *The Coandă Effect At Deflection Surfaces Widely Separated From The Jet Nozzle*, University of Toronto, Contract DA 44-177-AMC-11(T), USATRFCOM Technical Report 64-70, December 1964.
- [13] V. Dragan, A new mathematical model for high thickness Coanda effect wall jets, *Review of the Air Force Academy*, No 1 (23) 2013.
- [14] R. J. Englar, *Experimental Investigation Of The High Velocity Coanda Wall Jet Applied To Bluff Trailing Edge Circulation Control Airfoils*, Report 4708, September 1975.
- [15] D. S. Allen, *Axisymmetric Coanda-Assisted Vectoring*, Utah State University, Thesis Master of Science in Mechanical Engineering, 2008.
- [16] H. Alfredsson, R. Orlu, P. Schlatter, The viscous sublayer revisited-exploiting self-similarity it determine the wall position and friction velocity, *Experiments in Fluids*, ISSN: 0723-4864, ISSN: (Print) 1432-1114 (Online), Volume **51**, Iss.1, pp 271-280, doi: 10.1007/s00348-011-1048-8, 2011.
- [17] \* \* \* Numeca FINE™/Turbo v8.7 Flow Integrated Environment User Manual, May 2010, pag. 61.
- [18] M. R. Mendenhall, R. E. Childs, *Joseph H. Morrison, Best Practice Guidelines for Reduction of Uncertainty in the CFD Results (Invited)*, AIAA2004090091, 2004.
- [19] C. L. Rumsey and E. M. Lee-Rausch, *NASA Trapezoidal Wing Computations Including Transition and Advanced Turbulence Modeling, Conference Paper*, 30<sup>th</sup> AIAA Applied Aerodynamics Meeting; 25-28 Jun. 2012; New Orleans, LA; United States.
- [20] S. K. Arolla, P. A. Durbin, Modeling rotation and curvature effects within scalar eddy viscosity model framework, *International Journal of Heat and Fluid Flow*, ISSN: 0142-727X, Volume **39**, February 2013, Pages 78–89, DOI: 10.1016/j.ijheatfluidflow.2012.11.006
- [21] T. P. Dhakal and D. Keith Walters, A Three-Equation Variant of the SST  $k-\omega$  Model Sensitized to Rotation and Curvature Effects, *J. Fluids Eng.* ISSN: 0098-2202, eISSN: 1528-901X, Volume **133**, issue11, 111201, (9 pages), doi:10.1115/1.4004940, Oct 13, 2011.
- [22] Q. Zhang, Y. Yang, A new simpler rotation/curvature correction method for Spalart–Allmaras turbulence model, *Chinese Journal of Aeronautics*, ISSN: 1000-9361, Volume **26**, Issue 2, April 2013, Pages 326–333, DOI: 10.1016/j.cja.2013.02.009.
- [23] M. Trancossi, *An Overview of Scientific and Technical Literature on Coanda Effect Applied to Nozzles*, SAE Technical Paper 2011-01-2591, 2011, doi:10.4271/2011-01-2591.
- [24] Y. Xu, L.-H. Feng, J.-J. Wang, Experimental investigation of a synthetic jet impinging on a fixed wall, *Experiments in Fluids*, ISSN: 0723-4864, ISSN: (Print) 1432-1114 (Online, DOI 10.1007/s00348-013-1512-8, April 2013), 54:1512.
- [25] G. Krishnan, K. Mohseni, An experimental study of a radial wall jet formed by the normal impingement of a round synthetic jet, *European Journal of Mechanics - B/Fluids*, Volume **29**, Issue 4, Pages 69–277, DOI: 10.1016/j.euromechflu.2010.03.001, July–August 2010.